Rajshahi University journal of science and engineering **ISSN 2309-0952 (Print)**
Vol. 46-53 (2018-2025), pp 27-49 **ISSN 2408-8803 (Online)**
DOI: https://doi.org/10.64102/rujse.0764

Homotopy Perturbation Approach to Fractional-Order CAR T-Cell Therapy with Cytokines in Leukemia

Rezaul Karim[1*], M. A. Bkar Pk[2], Pinakee Dey[3], M. Ali Akbar[4]

Abstract

Leukemia is a type of blood cancer marked by the irregular proliferation of cells that originate in the bone marrow, representing a major global health concern. This research introduces a fractional-order (FO) five-compartment mathematical model for leukemia, which includes susceptible blood cells $s_1(t)$, infected blood cells $i_1(t)$, cancer cells $c_1(t)$, immune blood cells $w_1(t)$, and cytokine cells $c_2(t)$. The homotopy perturbation method (HPM) is employed to derive analytical solutions, whereas the fourth-order Runge-Kutta (RK4) method is utilized to calculate numerical solutions for the CAR-T cell therapy model. This model is structured to investigate the dynamics of the disease, and a comparative analysis is performed between the analytical and numerical outcomes. For the fractional parameter α = 0.45, The results demonstrate that the FO model provides higher accuracy and stability in contrast to the conventional integer-order model. Consequently, FO modeling is essential for comprehending leukemia dynamics and highlights the critical necessity for global access to this form of immunotherapy.

***Keywords**:* MM; HPM; RK4; CAR; and FO.

1. Introduction

In many practical fields, including science, engineering, biological systems, and economics, mathematical modeling and numerical simulation are frequently used to uncover the fundamental dynamics of real-world phenomena. In leukemia, abnormal blood cells can grow and proliferate more aggressively than healthy cells, gradually suppressing or disrupting the normal production of blood cells. By 2016, approximately 2.3 million individuals worldwide were living with leukemia, with an estimated 353,500 associated deaths (see Fig. 1) (Ferlay et al., 2015; Khatun & Biswas, 2020; Cancer Data, 2023; and Abdulla, F., & Nain, Z., 2021). To address the infection of CD4+ T-cells by HTLV-I, the HPM model has been detailed by Merdan, M. (2009). The HPM is uniformly valid, even for large parameters, and offers greater accuracy compared to the perturbation solutions reported by (He, 2003; S. T. & Noor, 2009). (Najafi & Basirzadeh, 2019) have obtained optimal control HPM for a cancer model, and the results obtained

[1] PhD Fellow, Department of Applied Mathematics, University of Rajshahi, Bangladesh
Assistant Professor, Department of Mathematics, Mawlana Bhashani Science and Technology University, Bangladesh, E-mail: rezaulmath11124@gmail.com * Corresponding Author
[2] Professor, Department of Applied Mathematics, University of Rajshahi, Bangladesh, E-mail: pkbakar@gmail.com
[3] Professor, Department of Mathematics, Mawlana Bhashani Science and Technology University, Bangladesh, E-mail: pinakeedey68@gmail.com
[4] Professor, Department of Applied Mathematics, University of Rajshahi, Bangladesh, E-mail: ali.akbar@ru.ac.bd

showed that the OCHPM method is powerful enough to generate the numerical solutions for some therapeutic models. (He, 2005) did describe the application of HPM to nonlinear wave equations. (Avazzadeh et al., 2023) have described that an enhanced cure may happen after the 2nd injection of CAR-T cells. To extend HPM with an auxiliary term by He (2012). Using an enhanced HPM has been described by Hossein et al. (2008).

Numerical and graphical results are obtained, demonstrating that the proposed scheme is computationally efficient, highly accurate, and straightforward to apply for analyzing and solving fractionally coupled nonlinear complex problems arising in science and technology (Ishag et al., 2022; Atangana, 2015; Adnan et al., 2022; Maayah and Arqub, 2023). MM of leukemia treatment with CAR T cell therapy and the immune system: the history and background of immunotherapy (Abbott & Ustoyev, 2019; Yang et al., 2015; Fadaei et al., 2021; Shah et al., 2024; Avazzadeh et al., 2023; Karim et al., 2024). (Modanli, 2022) has compared the Caputo and Atangana-Baleanu fractional derivatives for the pseudohyperbolic telegraph differential equations. (He, 1999) established the homotopy perturbation technique. Farman et al. (2024) presented a mathematical analysis and numerical simulations of a Zika virus model incorporating a time-fractional derivative. Baleanu et al. (2020) introduced a novel mathematical framework for modeling the human liver using the Caputo–Fabrizio fractional derivative.

In addition, Liao (1995) developed an approximate analytical solution method that does not rely on the presence of small parameters. Owolabi and Atangana (2017) investigated the formulation and application of a fractional Adams-Bashforth scheme based on the Caputo-Fabrizio derivative. Several studies have employed numerical and FO modeling approaches to analyze disease dynamics and treatment strategies. For instance, Karim et al. (2025a, 2025e) explored and predicted the COVID-19 epidemic in Bangladesh by numerical techniques, while Arefin et al. (2024) conducted a reasonable study of numerical approaches for solving ordinary differential equations. Fractional-order models have also been widely applied in cancer research, including studies on CAR T-cell therapy for leukemia using homotopy perturbation methods, Laplace-Adomian decomposition, and optimal control approaches (Karim et al., 2025b, 2025c, 2025d). In addition, Naik et al. (2025) investigated cancer treatment with radiotherapy using real data, and Singh et al. (2026) developed a Prabhakar fractional-order model for malaria transmission incorporating vaccination and waning immunity. Furthermore, Shah et al. (2025) proposed a fractional-order infectious disease model considering social media effects, highlighting the broad applicability of fractional modeling techniques

While many researchers have used the Caputo derivative to find approximate solutions for the model, we have applied the fractional beta derivative. In this study, we develop and analyze a mathematical model (MM) for leukemia, represented by a system of FO differential equations. The model consists of five compartmental components: Fractional order $s_1(t)$, $i_1(t)$, $c_1(t)$, $w_1(t)$, and $c_2(t)$. The objective of this study is to examine numerical solutions, graphical visualizations, constraint analyses, explanations, and solution behavior of the FO model using the RK4 method and the HPM. The HPM-obtained solution profiles are displayed and contrasted with the matching numerical solutions. The accuracy, ease of use, and effectiveness of the HPM are validated by this comparison study.

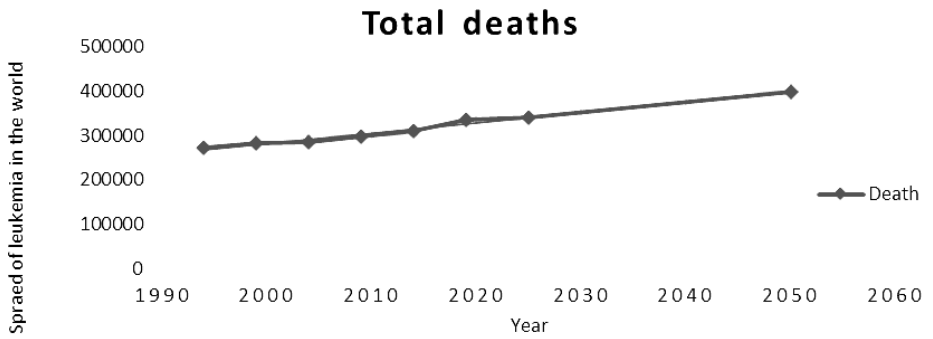

Figure 1: This study projects global death increases for the years 2025–2050 and looks at leukemia-related mortality data from 1994 to 2019.

2. Methods and Materials

The exploration of techniques involving symmetry and control systems represents a challenging but significant area within contemporary mathematical control theory and harmonic analysis. This field has a wide range of applications and attracts the attention of numerous researchers worldwide. T-cell therapy is an advanced form of immunotherapy that harnesses a patient's own immune cells to combat diseases, especially cancer. T-cells, a vital type of white blood cell, are responsible for detecting and eliminating abnormal or infected cells. In this treatment, T-cells are taken from the patient's blood, modified or multiplied in the laboratory to boost their ability to fight cancer, and then reinfused into the body, where they selectively target and destroy cancer cells.

The asymptotic fraction presents a serious risk because it can spread the disease to uninfected areas, but immunization rate and FO constraints are attractive parameters that have been defined by Jan et al. (2024). Pang and Z. (2016) proposed and analyzed a MM describing tumor conduct strategies involving pulsated immunotherapy combined with chemotherapy. Khan et al. (2020) have determined Laplace decomposition method (LADM) for solving nonlinear systems of FO partial differential equations. Kumar et al. (2014) have studied an analytical solution of the fractional Navier-Stokes equation by using the modified LADM. (Islam & Akbar, 2024) have also been investigated on the FO COVID-19 SEIQR model and parameter study by the HPM. HPM is particularly favored because it transforms complex nonlinear equations into a series of simpler, more manageable problems, making their solutions easier to obtain. The HPM is a powerful semi-analytical approach for solving nonlinear fractional differential equations (FDEs). It decomposes the solution into a series and avoids linearization and discretization, providing efficient and accurate results.

Step 1: To deliberate the HPM (He, 1999), we think about the succeeding nonlinear equation

$$F(x) - \varphi(\nu) = 0,\ u \in \Psi, \tag{2.1}$$

where, $$G\left(x, \frac{\partial x}{\partial r}\right) = 0,\ \nu \in \Gamma, \tag{2.2}$$

Step 2: Now, from equation (2.1) we get

$$P(x) + Q(x) - \varphi(\nu) = 0 \quad (2.3)$$

we make a homotopy then, by the HPM,

$$I(\nu, m): \zeta \times [0,1] \in R.$$

This satisfied

$$H(\nu, m) = (1 - m)\{P(I) - P(x_0)\} + m\{M(I) - \varphi(\nu)\} = 0, \quad (2.4)$$

or $$H(\nu, m) = P(I) - P(x_0) + mP(x_0) + m\{Q(I) - \varphi(\nu)\} = 0, \quad (2.5)$$

From (2.4) -(2.5), we can write

$$H(\nu, m) = P(I) - P(x_0), \quad (2.6)$$

or $$H(\nu, 1) = F(I) - \varphi(\nu). \quad (2.7)$$

Step 3: If the parameter m is assumed to be sufficiently small, then by applying the classical perturbation approach, the solutions of equations (2.4) and (2.5) may be expressed as power series expansions in terms of m

$$I = I_0 + I_1 m + I_2 m^2 + I_3 m^3 + \ldots \quad (2.8.)$$

Putting, $m = 1$ in equation (2.8), we can write

$$I = I_0 + I_1 m + I_2 m^2 + I_3 m^3 + \ldots$$

$$y = \lim_{m \to 1} I = I_0 + I_1 + I_2 + I_3 + \ldots \quad (2.9)$$

The series in equation (2.9) is convergent, with its rate of convergence influenced by the linear operator $M(c)$. The methodology is described in detail and illustrated, adapted from our previously published work (Karim et al., 2025b).

2.1. Compartmental Mathematical Model of Leukemia

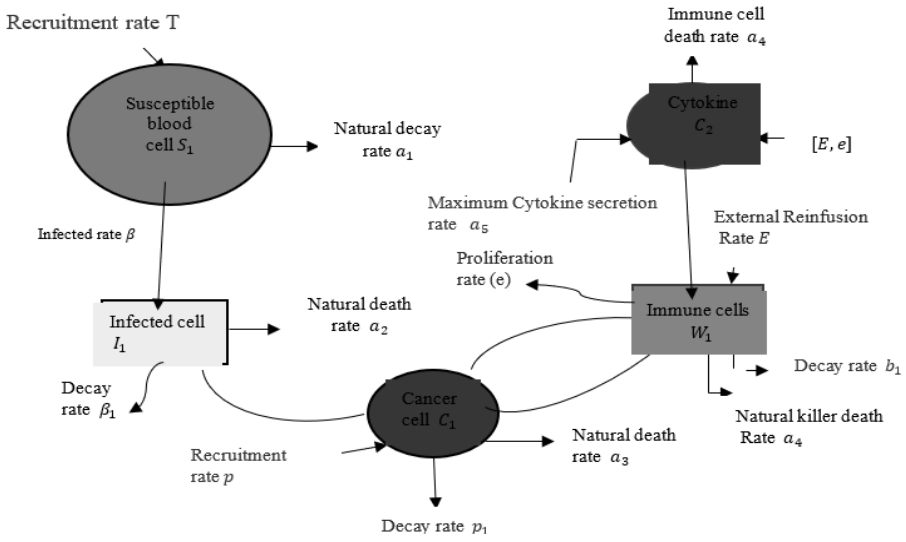

Fig. 2: Mathematical model of leukemia.

The constraints a_1, a_2, a_3, and a_4 denotes the natural death rates of $w_1(t)$ cells, $c_1(t)$ cells, $i_1(t)$ cells, and $s_1(t)$ blood cells, respectively. The parameter p_1 characterizes the rate at which cancer cells are eliminated through their interactions with immune cells. The schematic structure of the model is presented in Fig. 1 and is adapted from our previously published studies (Karim et al., 2025a, 2025b).

2.2. Estimation of Model Parameters

The parameter values in Table- 1 are from research done by (Khatun & Biswas, 2020; Cancer data, 2023; Khumaeroh et al., 2023).

Table 1: Purpose of the specific parameter of MM of leukemia

Parameters	Value	Dimension
T	1.5	$cells\mu l^{-1}d^{-1}$
a_1	0.01	d^{-1}
β	0.00005	$\mu cells\mu l^{-1}d^{-1}$
a_2	0.003	d^{-1}
β_1	0.005 or 0.001	$\mu cells\mu l^{-1}d^{-1}$
P	10	d^{-1}
a_3	5	d^{-1}
P_1	0.005	$\mu lcells^{-1}d^{-1}$
E	15	d^{-1}
e	0.01	
a_4	0.05	d^{-1}
b_1	0.001	$\mu lcells^{-1}d^{-1}$
a_5	0.0002	pg/ml
$s_1(t)$	149.079	
$i_1(t)$	1.082	
$c_1(t)$	900	
$w_1(t)$	252.26	
$c_2(t)$	20.00	

3. The solutions

According to the previous findings, the HPM only takes into account the first two terms of the series expansion while producing exact solutions. Adding more terms does not significantly improve accuracy; instead, it increases the algebraic complexity. The HPM proves to be particularly effective for nonlinear FO models and is simple to implement. In this research, the method is utilized to examine linear and nonlinear equations of leukemia MM, although it is typically used to derive approximate analytical solutions for both weakly and strongly nonlinear issues in science and engineering.

According to Khatun and Biswas (2020), Khumaeroh et al. (2023), and Karim et al. (2025b, 2025c) model, we considered as:

$$\left.\begin{aligned}
\frac{ds_1}{dt} &= T - a_1 s_1 - \beta s_1 c_1, \\
\frac{di_1}{dt} &= \beta s_1 c_1 - a_2 i_1 - \beta_1 c_1 i_1, \\
\frac{dc_1}{dt} &= p(1 - a_3 c_1)c1 - p_1 c_1 w_1, \\
\frac{dw_1}{dt} &= E + ec_1 - a_4 w_1 - b_1 w_1 c_1, \\
\frac{dc_2}{dt} &= (E + ec_1)a_5 - a_4 w_1 c_2,
\end{aligned}\right\} \qquad (3.1)$$

Equation (3.1) can be expressed as follows:

$$D_t^{\alpha} s_1(t) = T - a_1 s_1 - \beta s_1 c_1 \qquad (3.2)$$

$$D_t^{\alpha} i_1(t) = \beta s_1 c_1 - a_2 i_1 - \beta_1 c_1 i_1 \qquad (3.3)$$

$$D_t^{\alpha} c_1(t) = p(1 - a_3 c_1)c_1 - p_1 c_1 w_1 \qquad (3.4)$$

$$D_t^{\alpha} w_1(t) = E + ec_1 - a_4 w_1 - b_1 w_1 c_1 \qquad (3.5)$$

$$D_t^{\alpha} c_2(t) = (E + ec_1)a_5 - a_4 w_1 c_2 \qquad (3.6)$$

where, $s_1(t) > 0$, $i_1(t) \geq 0$, $c_1(t) \geq 0$, $w_1(t) \geq 0$, and $c_2(t) \geq 0$.

Here, several properties of the beta fractional derivative are presented and explained, adapted from our previously published study (Islam & Akbar, 2024). To transform the model into its conventional form, we let:

$$\mu = -\frac{\nu}{\alpha}\left(t + \frac{1}{\Gamma(\alpha)}\right)^{\alpha} \qquad (3.7)$$

Thus, $D_t^{\alpha} s_1(t) = \frac{\partial^{\alpha}}{\partial t^{\alpha}} S_1(\mu)$

$$= \frac{\partial S_1(\mu)}{\partial \mu}\frac{\partial^{\alpha}\mu}{\partial t^{\alpha}}$$

$$= -\frac{\nu}{\alpha} s_1'(\mu)\frac{\partial^{\alpha}}{\partial t^{\alpha}}\left\{\left(t + \frac{1}{\Gamma(\alpha)}\right)^{\alpha}\right\}$$

$$= -\frac{\nu}{\alpha} s_1'(\mu)\lim_{k\to 0}\frac{1}{k}[\{(t + \frac{1}{\Gamma(\alpha)}) + \alpha\left(t + \frac{1}{\Gamma(\alpha)}\right)^{\alpha-1} k\left(t + \frac{1}{\Gamma(\alpha)}\right)^{1-\alpha}$$

$$+ \ldots\} - \left(t + \frac{1}{\Gamma(\alpha)}\right)^{\alpha}]$$

$$= -\frac{\nu}{\alpha} s_1'(\mu)$$

Therefore, $D_t^{\alpha} s_1(t) = -\frac{\nu}{\alpha} s_1'(\mu)$ (3.8)

Similarly, $D_t^{\alpha} i_1(t) = -\frac{\nu}{\alpha} i_1'(\mu)$ (3.9)

$$D_t^{\alpha} c_1(t) = -\frac{\nu}{\alpha} c_1'(\mu) \quad (3.10)$$

$$D_t^{\alpha} w_1(t) = -\frac{\nu}{\alpha} w_1'(\mu) \quad (3.11)$$

$$D_t^{\alpha} c_2(t) = -\nu c_2'(\mu) \quad (3.12)$$

Using (3.8) -(3.12), from (3.2) - (3.6), we get

$$s_1'(\mu) = -\left(\frac{1}{\nu}\right)\{T - a_1 s_1(\mu) - \beta s_1(\mu)(c_1(\mu))\}, \quad (3.13)$$

$$i_1'(\mu) = -\left(\frac{1}{\nu}\right)\{\beta s_1(\mu) c_1(\mu) - a_2 i_1(\mu) - \beta c_1(\mu) i_1(\mu)\}, \quad (3.14)$$

$$c_1'(\mu) = -\left(\frac{1}{\nu}\right)\{p(1 - a_3 c_1(\mu)) c_1(\mu) - p_1 c_1(\mu) w_1(\mu)\}, \quad (3.15)$$

$$w_1'(\mu) = -\left(\frac{1}{\nu}\right)\{E + e c_1(\mu) - a_4 w_1(\mu) - b_1 w_1(\mu) c_1(\mu)\}, \quad (3.16)$$

$$c_2'(\mu) = -\left(\frac{1}{\nu}\right)\{\{E + e c_1(\mu)\} a_5 - a_4 w_1(\mu) c_2(\mu)\}, \quad (3.17)$$

Applying the HPM to equations (3.13)- (3.17), we obtain:

$$(1-p)\left\{s_1'(\mu) - \left(\frac{a_1}{\nu}\right) s_1(\mu)\right\} + p\left\{s_1'(\mu) + \left(\frac{T}{\nu}\right) - \left(\frac{a_1}{\nu}\right) s_1(\mu) - \left(\frac{\beta}{\nu}\right) s_1(\mu) c_1(\mu)\right\}, \quad (3.18)$$

$$(1-p)\left\{i_1'(\mu) - \left(\frac{a_2}{\nu}\right) i_1(\mu)\right\} + p\left\{i_1'(\mu) + \left(\frac{\beta}{\nu}\right) s_1(\mu) c_1(\mu) - \left(\frac{a_2}{\nu}\right) i_1(\mu) - \left(\frac{\beta_1}{\nu}\right)(c_1(\mu) i_1(\mu))\right\}, \quad (3.19)$$

$$(1-p)\{c_1'(\mu) - \left(\frac{a_3}{\nu}\right) c_1(\mu) + p\{c_1'(\mu) + \left(\frac{p}{\nu}\right)\{1 - a_3 c_1(\mu) c_1(\mu) - (\frac{p_1}{\nu}) c_1(\mu) w_1(\mu)\} \quad (3.20)$$

$$(1-p)\left\{w_1'(\mu) - \left(\frac{a_4}{\nu}\right) w_1(\mu)\right\} + p\left\{w_1'(\mu) + \left(\frac{E}{\nu}\right) + \left(\frac{e}{\nu}\right) c_1(\mu) - \left(\frac{a_4}{\nu}\right) w_1(\mu) - (\frac{b_1}{\nu}) w_1(\mu) c_1(\mu)\right\} \quad (3.21)$$

$$(1-p)\{c_2'(\mu) + p\{(c_2'(\mu) + (\frac{b_1}{\nu} + \frac{e}{\nu}(c_1(\mu)) a_5 - \frac{a_4}{\nu}(w_1(\mu) c_1(\mu) \quad (3.22)$$

and the conditions are:

$$s_1(0) = s_{10} = d_0, \qquad i_1(0) = i_{10} = d_1,$$

$$c_1(0) = c_{10} = d_2,\ w_1(0) = w_0 = d_3,\ c_2(0) = c_{20} = d_4. \tag{3.23}$$

and $$s_{1i}(0) = 0,\ i_{1i}(0) = 0,\ c_{1i}(0) = 0,\ w_{1i}(0) = 0,\ c_{2i}(0) = 0 \tag{3.24}$$

Consider the solutions of (3.18) - (3.22), we get

$$s_1(0)(\mu) = s_{10}(\mu) + ps_{11}(\mu) + p^2 s_{12}(\mu) + ... \tag{3.25}$$

$$i_1(0)(\mu) = i_{10}(\mu) + pi_{11}(\mu) + p^2 i_{12}(\mu) + ... \tag{3.26}$$

$$c_1(0)(\mu) = c_{10}(\mu) + pc_{11}(\mu) + p^2 c_{12}(\mu) + ... \tag{3.27}$$

$$w_1(0)(\mu) = w_{10}(\mu) + pw_{11}(\mu) + p^2 w_{12}(\mu) + ... \tag{3.28}$$

$$c_2(0)(\mu) = c_{20}(\mu) + pc_{21}(\mu) + p^2 c_{22}(\mu) + ... \tag{3.29}$$

Substituting solutions (3.25)-(3.29) into equations (3.18)-(3.22) and comparing the coefficients of like powers of p on both sides, we obtain

$$p^0 : -\left(\frac{1}{\nu}\right) a_1 s_{10}(\mu) + s_{10}'(\mu) = 0 \tag{3.30}$$

$$p^1 : \left(\frac{1}{\nu}\right)\{T - \beta i_{10}(\mu)s_{10}(\mu) - a_1 s_{11}(\mu) + \nu s_{11}'(\mu)\} = 0 \tag{3.31}$$

$$p^2 : -\left(\frac{1}{\nu}\right)\{\beta i_{11}(\mu)s_{10}(\mu) + \beta i_{10}(\mu)s_{11}(\mu) + a_1 s_{12}(\mu) - \nu s_{12}'(\mu)\} = 0 \tag{3.32}$$

$$p^0 : -\left(\frac{1}{\nu}\right)\{a_2 i_{10}(\mu) + i_{10}'(\mu) = 0 \tag{3.33}$$

$$p^1 : \left(\frac{1}{\nu}\right)\{- a_2 i_{11}(\mu) - \beta_1 i_{10}(\mu)c_{10}(\mu) + \beta c_{10}(\mu)s_{10}(\mu) + \nu i_{11}'(\mu)\} = 0 \tag{3.34}$$

$$p^2 : -\left(\frac{1}{\nu}\right)\{ - a_2 i_{12}(\mu) - \beta_1 i_{11}(\mu)c_{10}(\mu) - \beta_1 i_{10}(\mu)c_{11}(\mu) + \beta c_{11}(\mu)s_{10}(\mu) +$$

$$\beta c_{10}(\mu)s_{11}(\mu) + \nu i_{12}'(\mu)\} = 0 \tag{3.35}$$

$$p^0 : -\left(\frac{1}{\nu}\right)\{a_3 c_{10}(\mu) + c_{10}'(\mu) = 0 \tag{3.36}$$

$$p^1 : \left(\frac{1}{\nu}\right)\{- pi_{10}(\mu)^2 a_3 - c_{11}(\mu)a_3 + c_{10}(\mu)(p + a_3 - p_1 w_{10}(\mu) + \nu c_{11}'(\mu)\} = 0 \tag{3.37}$$

$$p^2 : \left(\frac{1}{\nu}\right)\{\{- a_3 c_{12}(\mu) - p_1 c_{11}(\mu)w_{11}(\mu)\} + c_{11}(\mu)\{p + (1 - 2pa_3 c_{10}(\mu) - p_1 w_{11}(\mu) +$$

$$\nu c_{12}'(\mu)\} = 0 \tag{3.38}$$

$$p^0 : -\left(\frac{1}{\nu}\right)\{\{a_4 c_{10}(\mu)\} + w_{10}'(\mu)\} = 0 \tag{3.39}$$

$$p^1 : \left(\frac{1}{\nu}\right)\{E - a_4 w_{11}(\mu) + c_{10}(\mu)\{e - w_{10}(\mu)b_1\} + \nu w_1'(\mu)\} = 0 \tag{3.40}$$

$$p^2 : \left(\frac{1}{\nu}\right)\{ - a_4 w_{12}(\mu) + b_1 c_{10}(\mu) w_{11}(\mu) + \{e - w_{10}(\mu)b_1\} + \nu w_{12}'(\mu)\} = 0 \tag{3.41}$$

$$p^0 : c_{20}'(\mu) \tag{3.42}$$

$$p^1 : \left(\frac{1}{\nu}\right)\{b_3 a_5 + a_5 e c_{10}(\mu) - w_{10}(\mu)c_{20}(\mu)c_{20}(\mu)a_4 + \nu c_{21}'(\mu)\} = 0 \tag{3.43}$$

$$p^2 : \left(\frac{1}{\nu}\right)\{- a_4 w_{11}(\mu)c_{20}(\mu) - b_3 c_{21}(\mu)w_{10}(\mu) + c_{11}(\mu)e + \nu c_{22}'(\mu)\} = 0 \tag{3.44}$$

Therefore, the answers to the aforementioned equations are:

$$s_{10}(\mu) = d_0 e^{\frac{a_1 \mu}{\nu}} \tag{3.45}$$

$$s_{11}(\mu) = \frac{T - e^{\frac{a_1 \mu}{\nu}} T}{a_1} + \frac{d_0 d_2 e^{\frac{a_1 \mu}{\nu}} (-1 + e^{\frac{\mu a_3}{\nu}})\beta}{a_3} \tag{3.46}$$

$$i_{10}(\mu) = d_1 e^{\frac{\gamma \mu}{\nu}} \tag{3.47}$$

$$i_{11}(\mu) = \frac{1}{a_3(-a_2 + a_3 + a_1)}\left(d_2 e^{\frac{a_2 \mu}{\nu}} \{-d_1(-1 + e^{\frac{\mu a_3}{\nu}})\beta_1(a_2 - a_1) + (-d_0(-1 + e^{\frac{\mu(-a_2 + a_1 + a_3)}{\nu}})\beta + d_1(-1 + e^{\frac{\mu a_3}{\nu}})\beta_1)a_3)\}\right) \tag{3.48}$$

$$c_{10}(\mu) = d_2 e^{\frac{\mu a_3}{\nu}} \tag{3.49}$$

$$c_{11}(\mu) = \left(\frac{1}{\nu a_4}\right)\left\{ d_2 e^{\frac{\mu a_3}{\nu}} (d_3(-1 + e^{\frac{\mu a_4}{\nu}})\nu p_1 - ((d_2 \nu - d_2 e^{\frac{\mu a_3}{\nu}} \nu + \mu)p + \mu a_3)a_4 \right\} \tag{3.50}$$

$$w_{10}(\mu) = d_3 e^{\frac{\mu a_4}{\nu}} \tag{3.51}$$

$$w_{11}(\mu) = -\frac{1}{a_3(a_3 - a_4)a_4}((-1 + e^{\frac{\mu a_4}{\nu}})a_3^2 b_3 + d_2 d_3 e^{\frac{\mu a_4}{\nu}}(-1 + e^{\frac{\mu a_3}{\nu}})a_4^2 b_1 + a_3 a_4(d_2(e^{\frac{\mu a_3}{\nu}} - e^{\frac{\mu a_4}{\nu}})e - (-1 + e^{\frac{\mu a_4}{\nu}})b_3 - d_2 d_3 e^{\frac{\mu a_4}{\nu}}(-1 + e^{\frac{\mu a_3}{\nu}})b_1))\} \tag{3.52}$$

$$c_{20}(\mu)=d_4 e^{\frac{\mu a_5}{\nu}} \quad (3.53)$$

$$c_{21}(\mu)=\{d_3 d_4(-1+e^{\frac{\mu a_4}{\nu}})-\frac{d_2(-1+e^{\frac{\mu a_3}{\nu}})e a_5}{a_3}-\frac{\mu a_5 E}{\nu}\} \quad (3.54)$$

According to the HPM, from (3.45)-(3.54), we attain

$$s_1(\mu)=\frac{T+e^{\frac{a_1\mu}{\nu}}(-T+a_1 d_0)}{a_1}+\frac{d_0 d_2 e^{\frac{a_1\mu}{\nu}}(-1+e^{\frac{\mu a_3}{\nu}})\beta}{a_3} \quad (3.55)$$

$$i_1(\mu)=d_1 e^{\frac{\gamma\mu}{\nu}}+\frac{1}{a_3(-a_2+a_3+a_1)}\Bigg(d_2 e^{\frac{a_2\mu}{\nu}}\{-d_1(-1+e^{\frac{\mu a_3}{\nu}})\beta_1(a_2-a_1)+(-d_0(-1+ e^{\frac{\mu(-a_2+a_1+a_3)}{\nu}})\beta+d_1(-1+e^{\frac{\mu a_3}{\nu}})\beta_1)a_3)\}\Bigg) \quad (3.56)$$

$$c_1(\mu)=d_2 e^{\frac{\mu a_5}{\nu}}+\left(\frac{1}{\nu a_4}\right)\left\{d_2 e^{\frac{\mu a_3}{\nu}}(d_3(-1+e^{\frac{\mu a_4}{\nu}})\nu p_1-((d_2\nu-d_2 e^{\frac{\mu a_3}{\nu}}\nu+\mu)p+\mu a_3)a_4\right\} \quad (3.57)$$

$$w_1(\mu)=\frac{1}{a_3(a_3-a_4)a_4}\{(a_3(-a_3E+(d_2 e^{\frac{\mu a_3}{\nu}}e+E)a_4)+e^{\frac{\mu a_4}{\nu}}(a_3^2(E-d_3a_4)+d_2d_3(-1+ e^{\frac{\mu a_3}{\nu}})a_4^2b_1-a_3a_4(d_2e+E-d_3a_4+d_2d_3(-1+e^{\frac{\mu a_3}{\nu}})b_1))\} \quad (3.58)$$

$$c_2(\mu)=d_4 e^{\frac{\mu a_5}{\nu}}+\{d_3d_4(-1+e^{\frac{\mu a_4}{\nu}})-\frac{d_2(-1+e^{\frac{\mu a_3}{\nu}})e a_5}{a_3}-\frac{\mu a_5 E}{\nu}\} \quad (3.59)$$

Therefore, the answers to the aforementioned this model are:

$$s_1(t)=\frac{T+e^{-\frac{a_1(t+\frac{1}{\Gamma(\alpha)})^\alpha}{\alpha}}(-\lambda+d_0a_1)}{a_1}+\frac{d_0d_2e^{-\frac{a_1(t+\frac{1}{\Gamma(\alpha)})^\alpha}{\alpha}}(-1+e^{\frac{(t+\frac{1}{\Gamma[\alpha]})^\alpha a_3}{\alpha}})\beta}{a_3}; \quad (3.60)$$

$$i_1(t)=e^{-\frac{a_2(t+\frac{1}{\Gamma(\alpha)})^\alpha}{\alpha}}\{d_1+\frac{1}{a_3(-a_2+a_3+a_1)}d_2(-d_1\left(-1+e^{-\frac{\left(t+\frac{1}{\Gamma(\alpha)}\right)^\alpha a_3}{\alpha}}\right)\beta_1(a_2-a_1)\}+ \{(-d_0\left(-1+e^{-\frac{\left(t+\frac{1}{\Gamma(\alpha)}\right)^\alpha(-a_2+a_3+a_1)}{\alpha}}\right)\beta\}+\{d_1(-1+e^{-\frac{\left(t+\frac{1}{\Gamma[\alpha]}\right)^\alpha 3}{\alpha}})\beta_1)a_3))\}; \quad (3.61)$$

$$c_1(t)=\frac{1}{\nu a_4}d_2e^{-\frac{(t+\frac{1}{\Gamma(\alpha)})^\alpha a_3}{\alpha}}\{(d_3(-1+e^{-\frac{(t+\frac{1}{\Gamma(\alpha)})^\alpha a_4}{\alpha}})\nu p_1+(\nu+d_2(-1+e^{-\frac{(t+\frac{1}{\Gamma[\alpha]})^\alpha a_3}{\alpha}})\nu p+ \frac{\nu p(t+\frac{1}{\Gamma(\alpha)})^\alpha}{\alpha}+\frac{\nu(t+\frac{1}{\Gamma[\alpha]})^\alpha a_3}{\alpha})a_4)\} \quad (3.62)$$

$$w_1(t)=\frac{1}{a_3(a_3-a_4)a_4}((a_3(-a_3E+(d_2e^{-\frac{(t+\frac{1}{\Gamma(\alpha)})^\alpha a_1}{\alpha}}e+E)a_4)+e^{-\frac{(t+\frac{1}{\Gamma[\alpha]})^\alpha a_4}{\alpha}}(a_3^2E- d_3a_4)+d_2d_3(-1+e^{-\frac{(t+\frac{1}{\Gamma(\alpha)})^\alpha a_3}{\alpha}})a_4^2b_1-a_1a_4(d_2e+E-d_3a_4+d_2d_3(-1+ e^{-\frac{(t+\frac{1}{\Gamma[\alpha]})^\alpha a_1}{\alpha}})b_1))); \quad (3.63)$$

$$c_2(t)=d_4e^{-\frac{(t+\frac{1}{\Gamma(\alpha)})^\alpha a_5}{\alpha}}+d_3d_4(-1+e^{-\frac{(t+\frac{1}{\Gamma(\alpha)})^\alpha a_4}{\alpha}}-\frac{d_2\left(-1+e^{-\frac{(t+\frac{1}{\Gamma(\alpha)})^\alpha a_3}{\alpha}}\right)ea_5}{a_3}+ \frac{\left(t+\frac{1}{\Gamma(\alpha)}\right)^\alpha b_3a_5}{\alpha} \quad 3.64)$$

4. Results and Discussion

This section provides a comparison between the exact solutions of the FO CAR-T cell therapy model for leukemia obtained using the HPM and the numerical solutions computed via the RK4 method. To highlight the effects of different system parameters, we employ a numerical framework to examine the solution paths of the FO model. The outcomes from the HPM are compared with the numerical simulations to assess the accuracy and reliability of the analytical approach. By analyzing the plots from both methods, we can interpret the temporal dynamics of blood cell populations. Specifically, the graphs illustrate the behavior of susceptible blood cells $s_1(t)$, infected blood cells $i_1(t)$, cancer cells $c_1(t)$,immune blood cells $w_1(t)$, and cytokine cells $c_2(t)$. According to (Khatun & Biswas, 2020; Cancer data, 2023; Khumaeroh et al., 2023) From Eqs.(3.1), we assume the values

T = 1.5, a_1 = 0.01, β = 0.00005, a_2 = 0.003, β_1 = 0.005, p = 10, a_3 = 5, p_1 = 0.005, E = 15, e = 0.01, a_4 = 0.05, b_1 = 0.001, ν = –1.

Simulations were performed for a fixed duration of 100 days, and the results are presented in Figs. 3-7 below:

4.1. Comparison of the analytical and numerical approaches for tracking $s_1(t)$, $i_1(t)$, $c_1(t)$, $w_1(t)$, and $c_2(t)$.

Fig. 3 illustrates both the analytical and numerical results for $s_1(t)$ blood cells, analyzed across different values of the fractional-order parameter α.

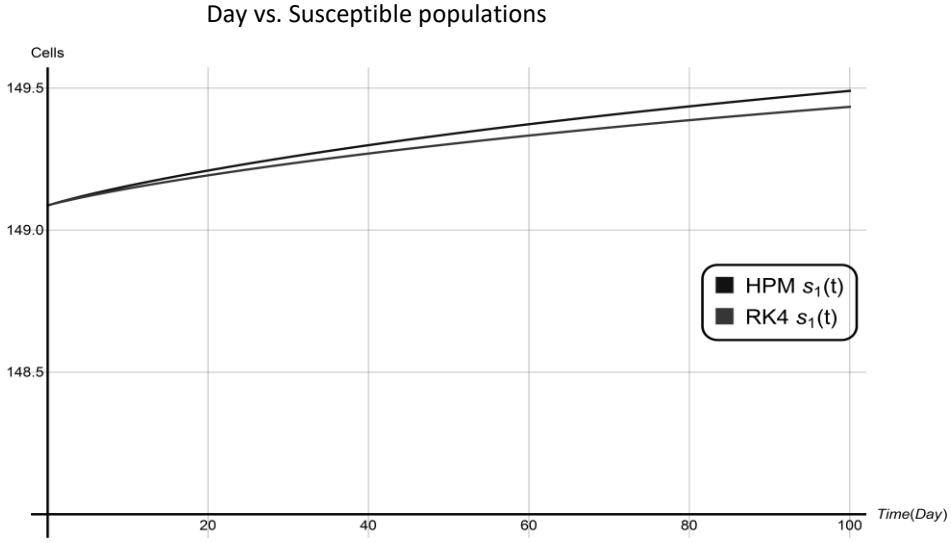

Fig. 3(a): Comparison of HPM and RK4 results for $s_1(t)$ over 0-100 days, with the FO parameter α = 1.00.

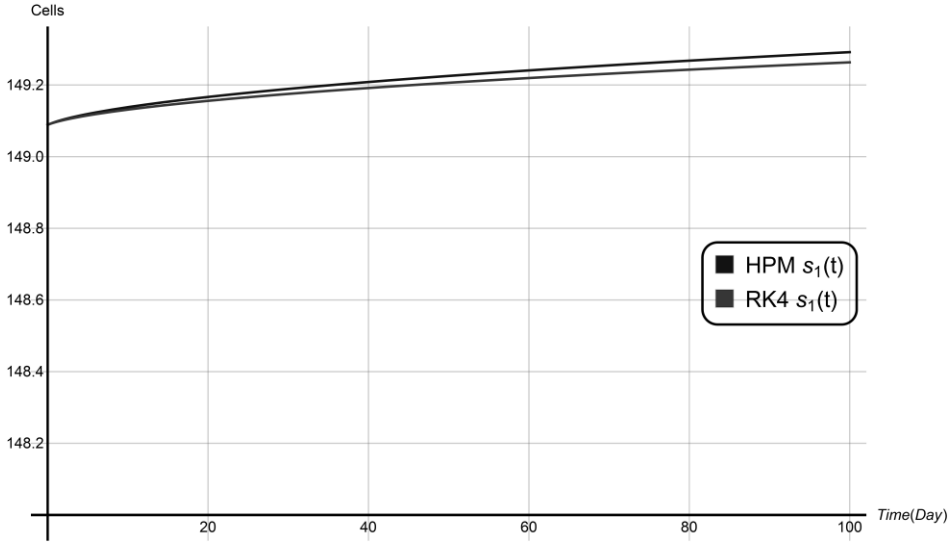

Fig. 3(b): Comparison of HPM and RK4 results for $s_1(t)$ over 0-100 days, with the FO parameter α = 0.90

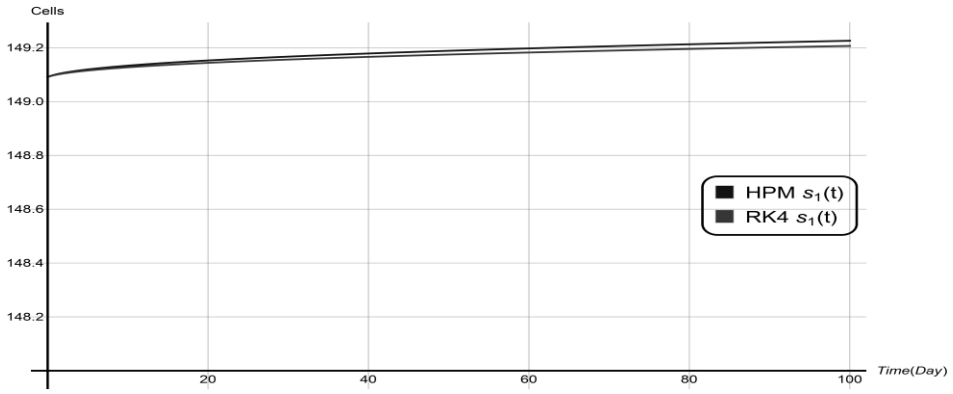

Fig. 3(c): Comparison of HPM and RK4 results for $s_1(t)$ over 0-100 days, with the FO parameter $\alpha = 0.75$.

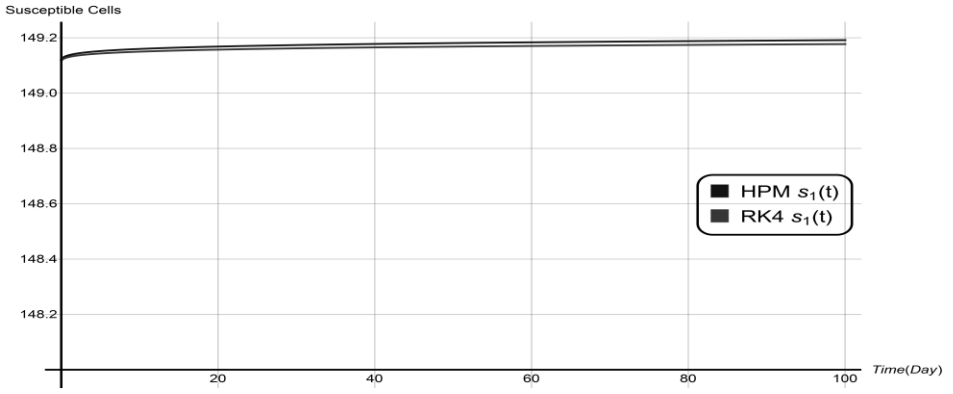

Fig. 3(d): Comparison of HPM and RK4 results for $s_1(t)$ over 0-100 days, with the FO parameter $\alpha = 0.60$.

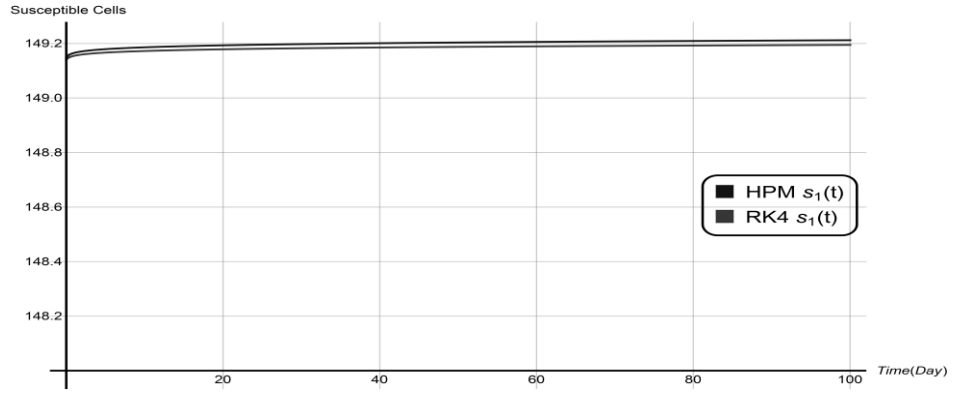

Fig. 3(e): Comparison of HPM and RK4 results for $s_1(t)$ over 0-100 days, with the FO parameter $\alpha = 0.45$.

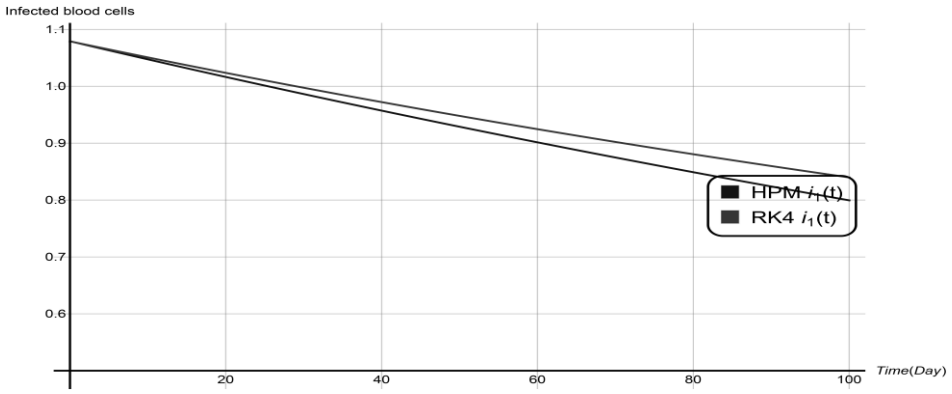

Fig. 4(a): Comparison of HPM and RK4 results for $i_1(t)$ over 0-100 days, with the FO parameter α = 1.0.

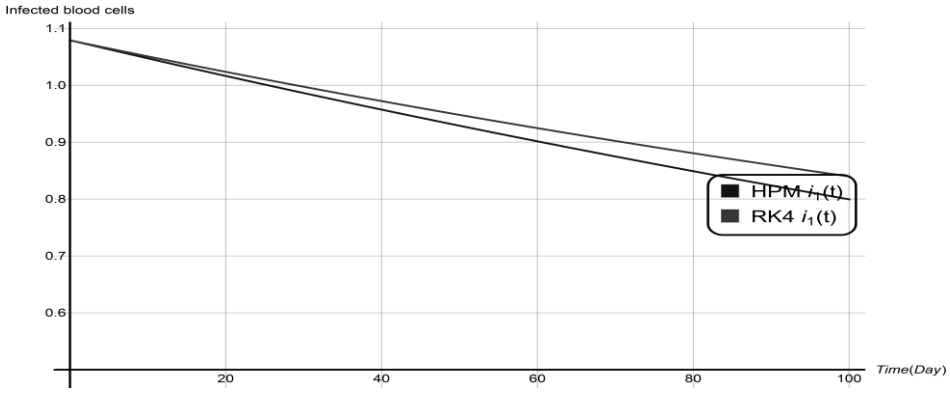

Fig. 4(b): Comparison of HPM and RK4 results for $i_1(t)$ over 0-100 days, with the FO parameter α = 0.90

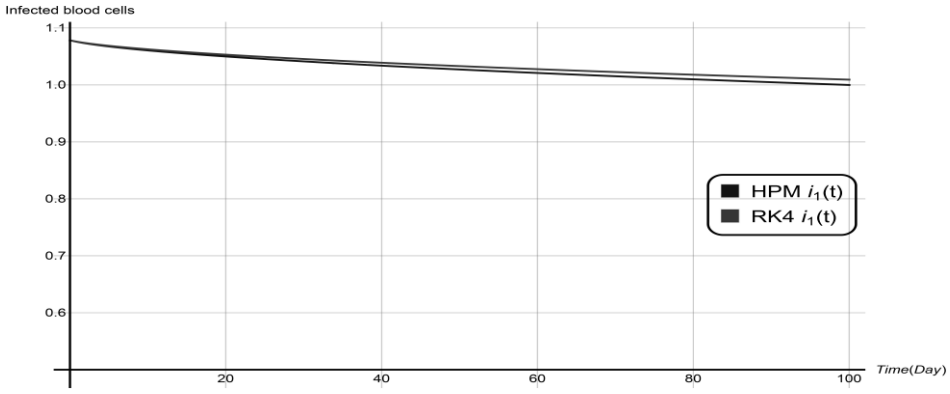

Fig. 4(c): Comparison of HPM and RK4 results for $i_1(t)$ over 0-100 days, with the FO parameter α = 0.75.

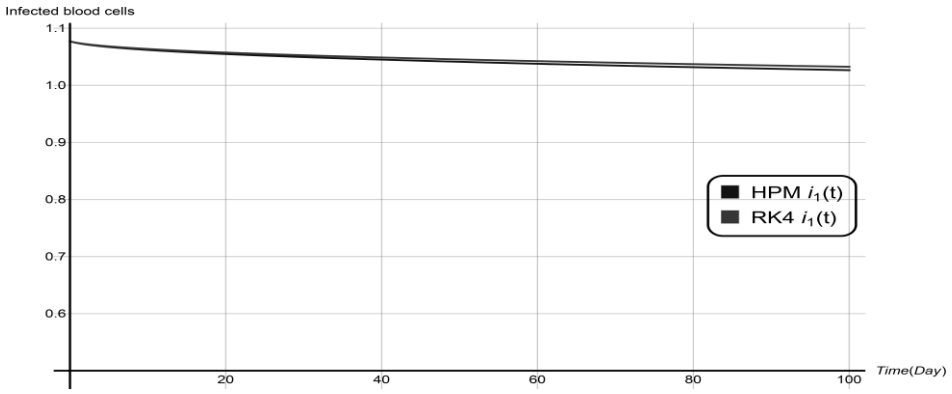

Fig. 4(d): Comparison of HPM and RK4 results for $i_1(t)$ over 0-100 days, with the FO parameter $\alpha = 0.60$..

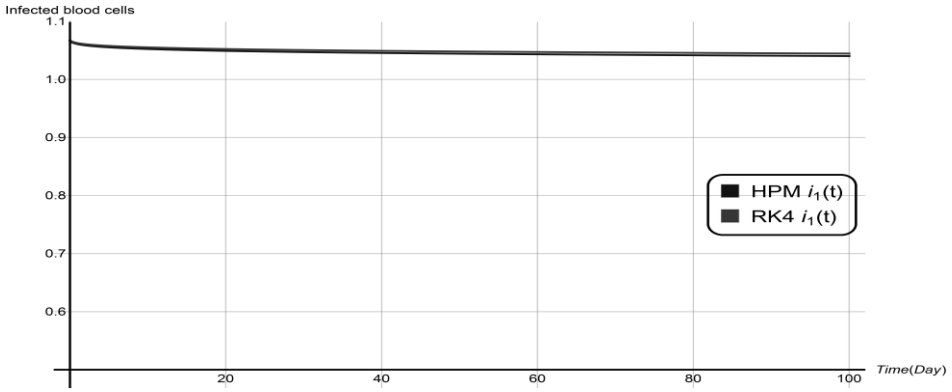

Fig. 4(e): Comparison of HPM and RK4 results for $i_1(t)$ over 0-100 days, with the FO parameter $\alpha = 0.45$.

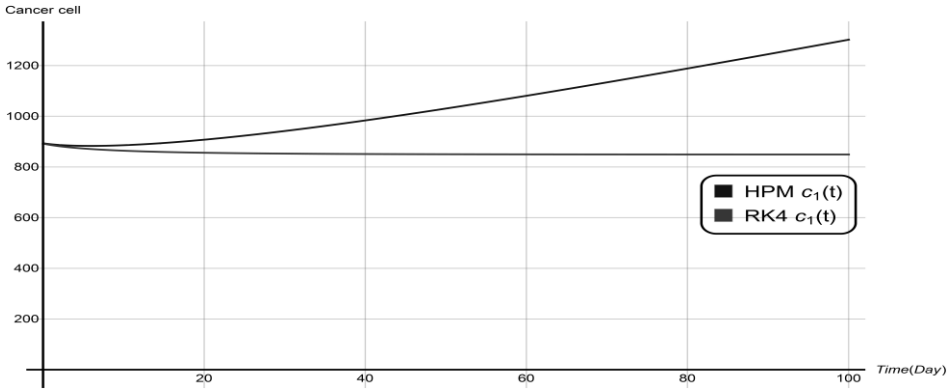

Fig. 5(a): Comparison of HPM and RK4 results for $c_1(t)$ over 0-100 days, with the FO parameter $\alpha = 1.0$.

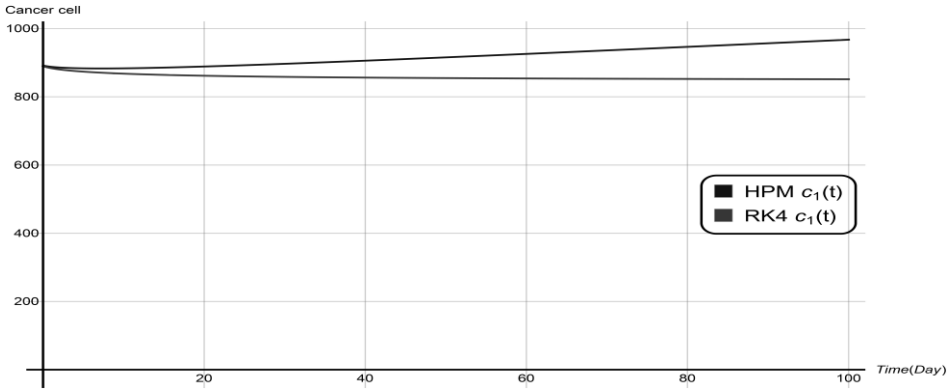

Fig. 5(b): Comparison of HPM and RK4 results for $c_1(t)$ over 0-100 days, with the FO parameter α = 0.90.

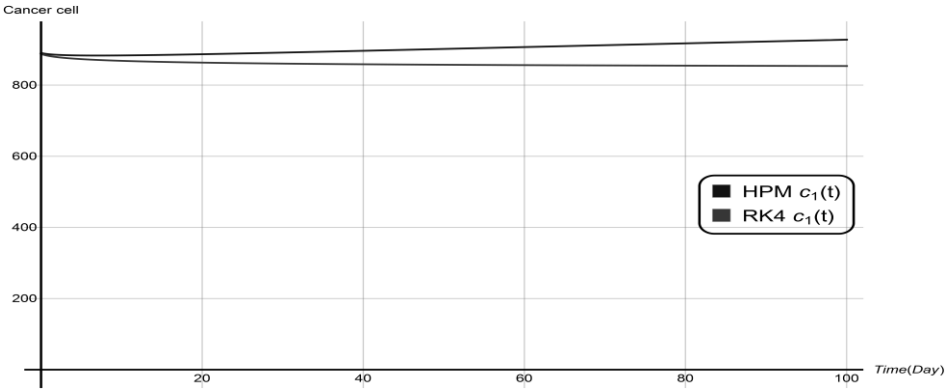

Fig. 5(c): Comparison of HPM and RK4 results for $c_1(t)$ over 0-100 days, with the FO parameter α = 0.75.

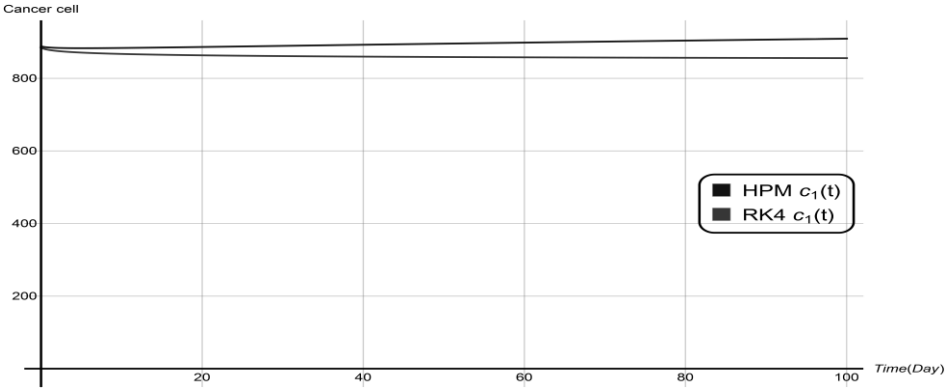

Fig. 5(d): Graph comparing the HPM and RK4 results for the cancer blood cells $c_1(t)$ over a time span of 0 to 100 days, with a parameter value of α = 0.60.

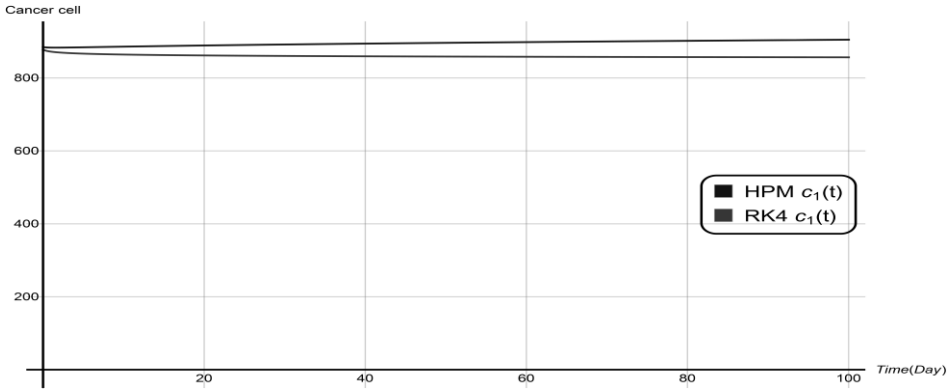

Fig. 5(e): Comparison of HPM and RK4 results for $c_1(t)$ over 0-100 days, with the FO parameter $\alpha = 0.60$.

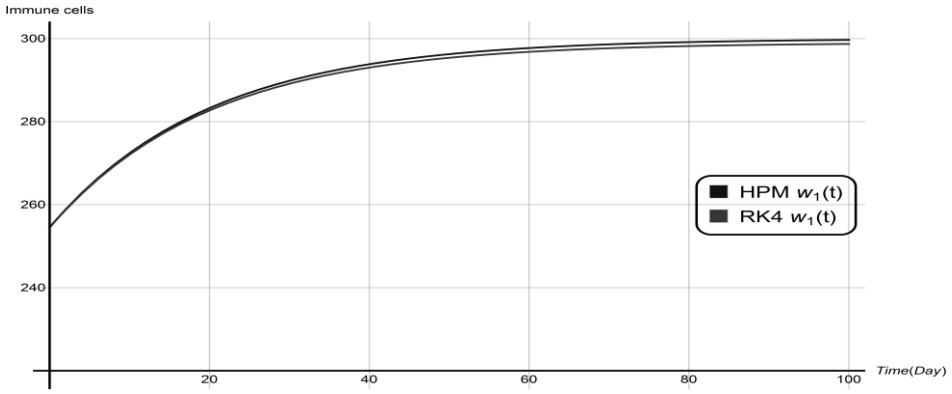

Fig. 6(a): Comparison of HPM and RK4 results for $w_1(t)$ over 0-100 days, with the FO parameter $\alpha = 1.0$.

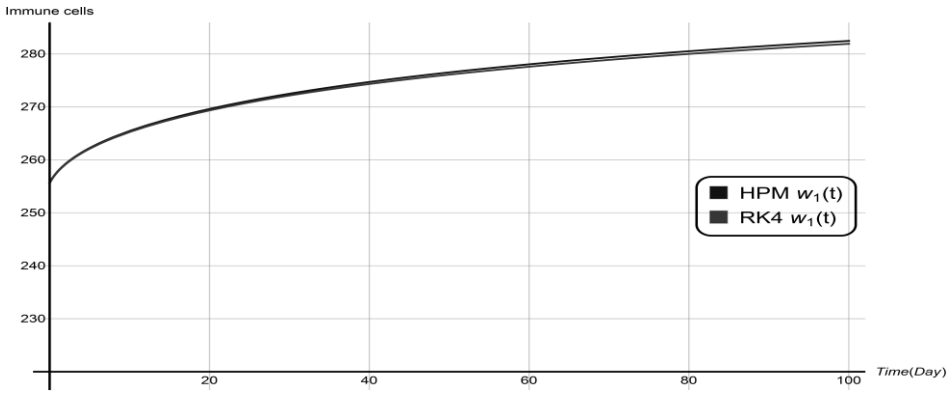

Fig. 6(b): Comparison of HPM and RK4 results for $w_1(t)$ over 0-100 days, with the FO parameter $\alpha = 0.90$.

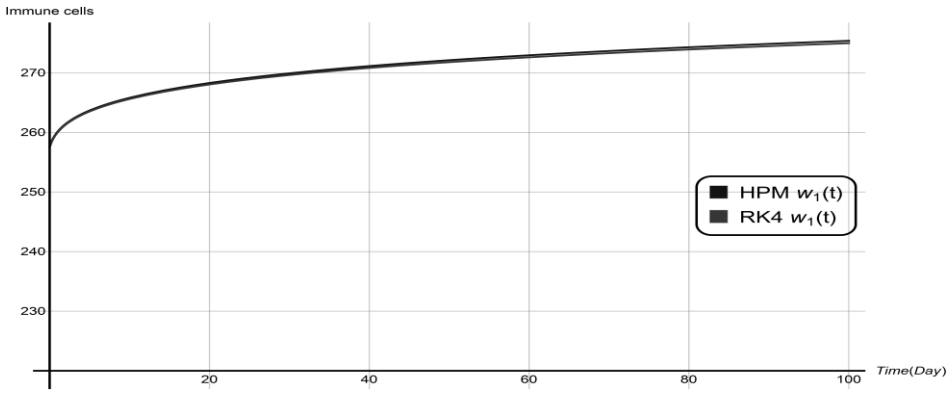

Fig. 6(c): Comparison of HPM and RK4 results for $w_1(t)$ over 0-100 days, with the FO parameter $\alpha = 0.75$.

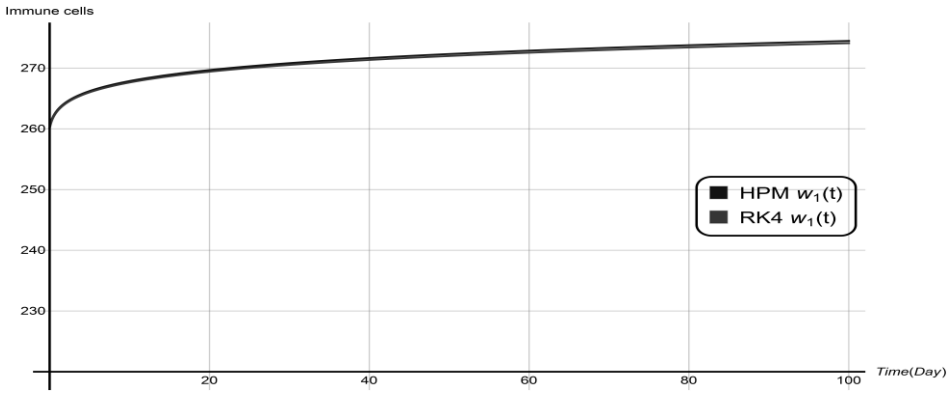

Fig.6(d): Comparison of HPM and RK4 results for $w_1(t)$ over 0-100 days, with the FO parameter $\alpha = 0.60$.

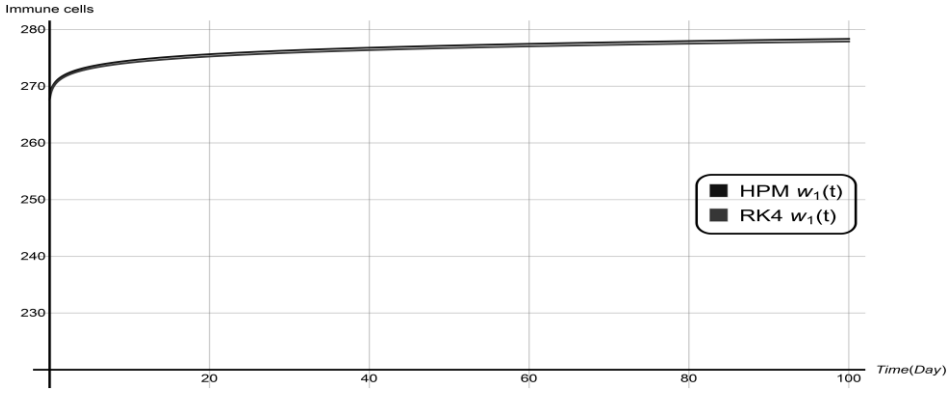

Fig. 6(e): Comparison of HPM and RK4 results for $w_1(t)$ over 0-100 days, with the FO parameter $\alpha = 0.45$.

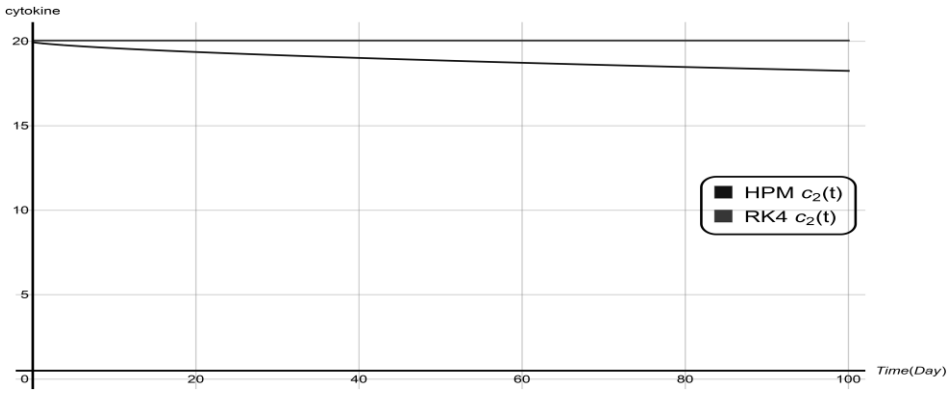

Fig. 7(a): Comparison of HPM and RK4 results for $c_2(t)$ over 0-100 days, with the FO parameter $\alpha = 1.0$

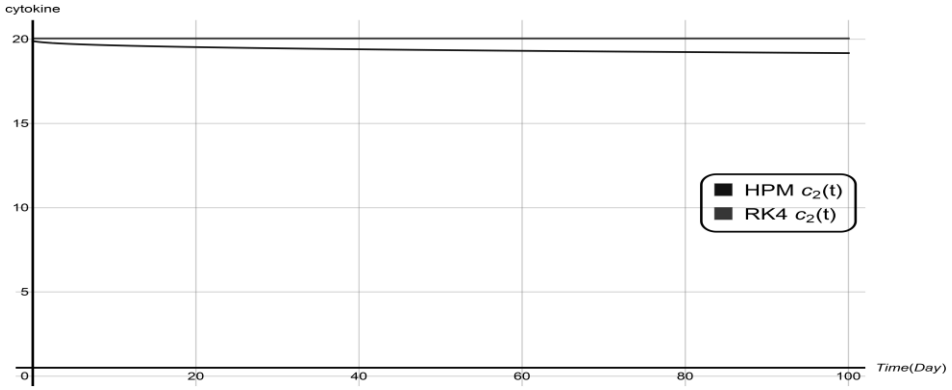

Fig. 7(b): Comparison of HPM and RK4 results for $c_2(t)$ over 0-100 days, with the FO parameter $\alpha = 0.90$.

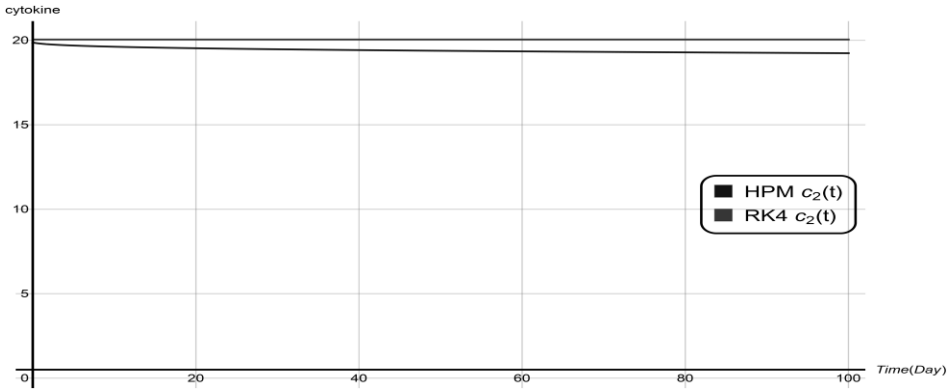

Fig. 7(c): Comparison of HPM and RK4 results for $c_2(t)$ over 0-100 days, with the FO parameter $\alpha = 0.75$

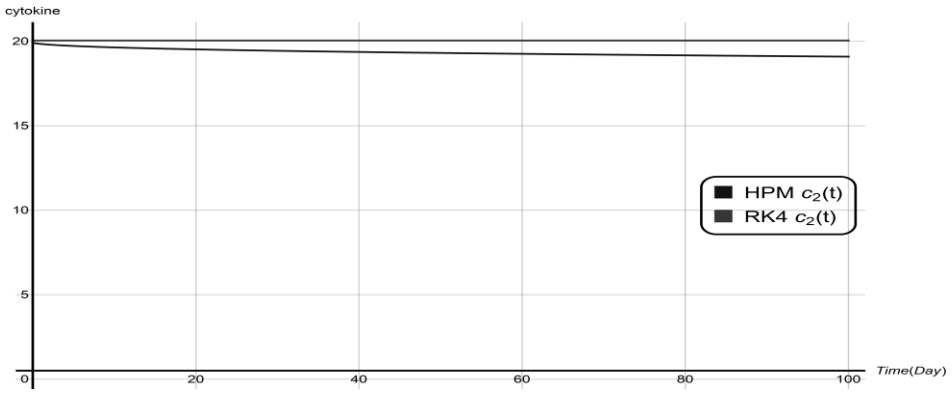

Fig. 7(d): Comparison of HPM and RK4 results for $c_2(t)$ over 0-100 days, with the FO parameter $\alpha = 0.75$

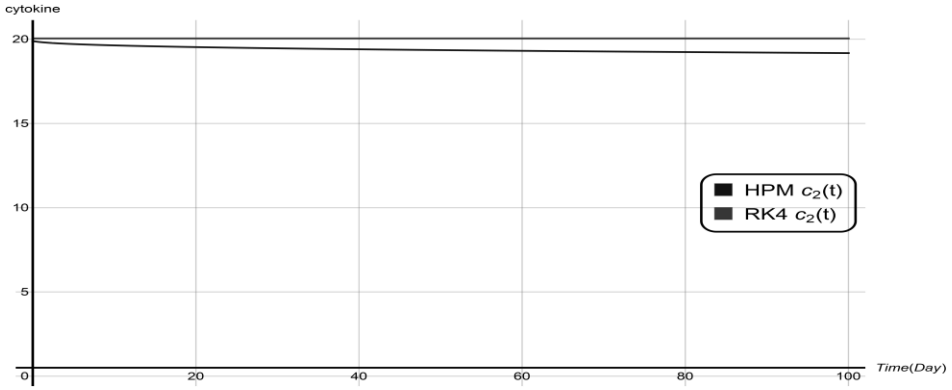

Fig. 7(e): Comparison of HPM and RK4 results for $c_2(t)$ over 0-100 days, with the FO parameter $\alpha = 0.45$.

Fig. 3(a) is plotted for $\alpha = 1$, representing the model's consistency with classical approaches. The red curve depicts the numerical solutions obtained via the RK4 method, while the blue curve represents the analytical solutions derived using HPM. According to Khatun and Biswas (2020), Cancer Data (2023), and Khumaeroh et al. (2023), the number of $s_1(t)$ cells is approximately 149.079. Figures 3(b)-(e) present a comparison of analytical and numerical solutions for $s_1(t)$ over 0-100 days, with FO values $\alpha = 0.90$, 0.75, 0.60, and 0.45, respectively. In all cases, HPM and RK4 solutions coincide at day 0, but the difference gradually increases toward day 100, with the closest agreement observed at $\alpha = 0.45$. The number of $s_1(t)$ decreases as $i_1(t)$ rise, reaching a highest around day 100 after disease onset. As immune cell counts improve, infection rates decline, stabilizing susceptible cell numbers and limiting leukemia progression. Higher cancer cell recruitment rates lead to increased numbers of cancerous and infected cells, causing more $s_1(t)$ to become $i_1(t)$ and resulting in a significant presence of abnormal, immature white blood cells that can develop into cancer.

Similarly, Figs. 4-7 demonstrate the comparisons between the analytical and numerical solutions for $i_1(t)$, $c_1(t)$, $w_1(t)$, and $c_2(t)$ across the time length of 0-100 days for the values of α = 1.00, 0.90, 0.75, 0.60, and 0.45, respectively. It is clear from Figs 4-7 that the analytical and numerical solutions show the greatest alignment when α = 0.45. In every instance, both solution methods coincide at the starting point (day 0), and the trends continue to be similar as time advances. Importantly, the outcomes associated with α = 0.45, reveal enhanced precision and greater consistency in comparison to the other fractional-order values.

5. Conclusion and Future Work

In this study, we examined the FO at the MM and parameter evaluation for leukemia using the HPM and the RK4 method. The parameters were chosen according to the behaviors of leukemia transmission, enabling us to examine a model that includes FO derivatives for a more comprehensive and flexible method of simulating the system's dynamics. Analytical solutions obtained through the HPM were in close agreement with numerical outcomes derived from the RK4 method, thereby validating the precision of the approach. Our results demonstrate that the analytical solutions derived using the HPM closely match the numerical solutions obtained through the RK4 method. An analysis across various FOs (α = 1.00, α = 0.90, α = 0.75, α = 0.60 and α = 0.45) suggests that the model makes optimally at α = 0.45, implying that lower FOs may better capture the dynamics of leukemia. When it came to solving complicated FO differential models, HPM outperformed conventional methods by offering reliable first and second-order approximations. In general, FO modeling provides a precise and adaptable framework for researching leukemia treatment. To make the model more applicable in the real world, future research may expand it by incorporating elements like vaccination tactics and novel disease variations.

Reference

Abbott, M., & Ustoyev, Y. (2019). Cancer and the immune system: the history and background of immunotherapy. In Seminars in oncology nursing (Vol. 35, No. 5, p. 150923). WB Saunders.

Abdulla, F., Nain, Z., Karimuzzaman, M., Hossain, M. M., & Rahman, A. (2021). A non-linear biostatistical graphical modeling of preventive actions and healthcare factors in controlling COVID-19 pandemic. International Journal of Environmental Research and Public Health, 18(9), 4491.

Adnan, Ali, A., ur Rahmamn, M., Shah, Z., & Kumam, P. (2022). Investigation of a time-fractional covid-19 mathematical model with singular kernel. Advances in Continuous and Discrete Models, 2022(1), 34.

Atangana, A. (2015). Derivative with a new parameter: theory, methods and applications. Academic Press.

Arefin, M. A., Gain, B., Karim, R., & Hossain, S. (2020). A comparative exploration on different numerical methods for solving ordinary differential equations. J. Mech. Cont. & Math. Sci, 15(12), 1-11.

Avazzadeh, Z., Hassani, H., Ebadi, M. J., Zarei-Behjani, Z., Bayati Eshkaftaki, A., Mehrabi, S., & Haghighat, S. (2023). Generalized Lerch polynomials: application in fractional model of CAR-T cells for T-cell leukemia. The European Physical Journal Plus, 138(12), 1152.

Baleanu, D., Jajarmi, A., Mohammadi, H., & Rezapour, S. (2020). A new study on the mathematical modelling of human liver with Caputo–Fabrizio fractional derivative. Chaos, Solitons & Fractals, 134, 109705.

https://Our World in Data.org/ Cancer. Acccesed march 2023.

Fadaei, Y., Ahmadi, A., Fekri, K., Masoumi, R., & Radunskaya, A. (2021). A fractional-order model for chronic lymphocytic leukemia and immune system interactions. Mathematical Methods in the Applied Sciences, 44(1), 391-406.

Farman, M., Ahmad, A., Akgül, A., Saleem, M. U., Rizwan, M., & Ahmad, M. O. (2024). A mathematical analysis and simulation for Zika virus model with time fractional derivative. Mathematical Methods in the Applied Sciences, 47(13), 11135-11146.

Ferlay, J., Soerjomataram, I., Dikshit, R., Eser, S., Mathers, C., Rebelo, M., ... & Bray, F. (2015). Cancer incidence and mortality worldwide: sources, methods and major patterns in GLOBOCAN 2012. International journal of cancer, 136(5), E359-E386.

He, J. H. (1999). Homotopy perturbation technique. Computer methods in applied mechanics and engineering, 178(3-4), 257-262.

He, J. H. (2003).Homotopy perturbation method: a new nonlinear analytical technique. Applied Mathematics and computation, 135(1), 73-79.

He, J. H. (2005). Application of homotopy perturbation method to nonlinear wave equations. Chaos, Solitons & Fractals, 26(3), 695-700.

He, J. H. (2012). Homotopy perturbation method with an auxiliary term. In Abstract and Applied Analysis (Vol. 2012, No. 1, p. 857612). Hindawi Publishing Corporation.

HosseinNia, S. H., Ranjbar, A., & Momani, S. (2008). Using an enhanced homotopy perturbation method in fractional differential equations via deforming the linear part. Computers & Mathematics with Applications, 56(12), 3138-3149.

Ishag, K. A., Abdallah, M. A., & Ahmed, A. M. (2022). Homotopy Perturbation Method for Solving Nonlinear Fractional Reaction Diffusion Systems. Applied and Computational Mathematics, 13(4), 48-55.

Jan, R., Hinçal, E., Hosseini, K., Razak, N. N. A., Abdeljawad, T., & Osman, M. S. (2024). Fractional view analysis of the impact of vaccination on the dynamics of a viral infection. Alexandria Engineering Journal, 102, 36-48.

Karim, R., Pk, M. B., Dey, P., Akbar, M. A., & Osman, M. S. (2024). A study about the prediction of population growth and demographic transition in Bangladesh. Journal of Umm Al-Qura University for Applied Sciences, 1-13.

Karim, R., Akbar, M. A., Miah, S. S., Pk, M. B., Dey, P., & Osman, M. S. (2025a). Exploration and prediction of COVID-19 pandemic in Bangladesh using numerical approach. Discover Data, 3(1), 13.

Karim, R., Akbar, M. A., Pk, M. B., & Dey, P. (2025b). A study on fractional-order mathematical and parameter analysis for CAR T-cell therapy for leukemia using homotopy perturbation method. Partial Differential Equations in Applied Mathematics, 14, 101152.

Karim, R., Akbar, M. A., Pk, M. B., Dey, P., & Tahmed, M. T. (2025c). Mathematical analysis of chimeric antigen receptor T-cell therapy for leukaemia using optimal control approach. Journal of Umm Al-Qura University for Applied Sciences, 1-18.

Karim, R., Akbar, M. A., Pk, M. B., &Dey, P.,(2025d). A study on numerical solutions of a fractional-order model for CAR T-cell therapy in leukemia using the Laplace-Adomian decomposition method, Sigma J Eng Nat Sci. (2025). doi: 10.14744/sigma.2025.00053

Karim, R., Pk, M. B., Akbar, M. A., & Dey, P. (2025e). A study on fractional-order mathematical analysis for inspecting the spread of the leukemia virus. Partial Differential Equations in Applied Mathematics, 101297.

Khatun, M. S., & Biswas, M. H. A. (2020). Modeling the effect of adoptive T cell therapy for the treatment of leukemia. Computational and Mathematical Methods, 2(2), e1069.

Khan, H., Shah, R., Kumam, P., Baleanu, D., & Arif, M. (2020). Laplace decomposition for solving nonlinear system of fractional order partial differential equations. Advances in Difference Equations, 2020, 1-18.

Khumaeroh, M. S., Shalehah, M. A., & Ilahi, F. (2023). Mathematical Model of Leukemia Treatment with Chimeric Antigen Receptor (CAR) T Cell Therapy. Mathline: Jurnal Matematika dan Pendidikan Matematika, 8(3), 1077-1090.

Kumar, S., Kumar, D., Abbasbandy, S., & Rashidi, M. M. (2014). Analytical solution of fractional Navier–Stokes equation by using modified Laplace decomposition method. Ain Shams Engineering Journal, 5(2), 569-574.

Liao, S. J. (1995). An approximate solution technique not depending on small parameters: a special example. International Journal of Non-Linear Mechanics, 30(3), 371-380.

Maayah, B., & Arqub, O. A. (2023). Hilbert approximate solutions and fractional geometric behaviors of a dynamical fractional model of social media addiction affirmed by the fractional Caputo differential operator. Chaos, Solitons & Fractals: X, 10, 100092.

Merdan, M. (2009). Homotopy perturbation method for solving human T-cell lymphotropic virus I (HTLV-I) infection of CD4+ T-cells model. Mathematical and Computational Applications, 14(2), 85-96.

Mohyud-Din, S. T., & Noor, M. A. (2009). Homotopy perturbation method for solving partial differential equations. Zeitschrift für Naturforschung A, 64(3-4), 157-170.

Modanli, M. (2022). Comparison of Caputo and Atangana–Baleanu fractional derivatives for the pseudohyperbolic telegraph differential equations. Pramana, 96(1), 7.

Najafi, M., & Basirzadeh, H. (2019). Optimal control homotopy perturbation method for cancer model. International Journal of Biomathematics, 12(03), 1950027.

Naik, P. A., Farman, M., Jamil, S., Saleem, M. U., Nisar, K. S., & Huang, Z. (2025). Modeling and computational study of cancer treatment with radiotherapy using real data. PLoS One, 20(5), e0320906.

Owolabi, K. M., & Atangana, A. (2017). Analysis and application of new fractional Adams–Bashforth scheme with Caputo–Fabrizio derivative. Chaos, Solitons & Fractals, 105, 111-119.

Pang, L., Shen, L., & Zhao, Z. (2016). Mathematical modelling and analysis of the tumor treatment regimens with pulsed immunotherapy and chemotherapy. Computational and Mathematical Methods in Medicine, 2016(1), 6260474.

Singh, A., Raval, R., Chavada, A., Pathak, N., & Pandey, R. K. (2026). Prabhakar fractional-order modeling of malaria transmission with vaccination and waning immunity. Franklin Open, 100484.

Shah, K., Abdeljawad, T., & Ali, Z. (2025). Mathematical model and simulations of fractional order for an infectious disease involving social media. Modeling Earth Systems and Environment, 11(6), 1-16.

Shah, K., Ahmad, S., Ullah, A., & Abdeljawad, T. (2024). Study of chronic myeloid leukemia with T-cell under fractal-fractional order model. Open Physics, 22(1), 20240032.

Song, F., Xu, C., & Karniadakis, G. E. (2017). Computing fractional Laplacians on complex-geometry domains: algorithms and simulations. SIAM Journal on Scientific Computing, 39(4), A1320-A1344.

Yang, X. J., Srivastava, H. M., & Cattani, C. (2015). Local fractional homotopy perturbation method for solving fractal partial differential equations arising in mathematical physics. Romanian Reports in Physics, 67(3), 752-761.